18

Qualitative Elemental Analysis by Energy Dispersive X-Ray Spectrometry

J. Goldstein et al., *Scanning Electron Microscopy and X-Ray Microanalysis*,
https://doi.org/10.1007/978-1-4939-6676-9_18

■■ Overview

Qualitative elemental analysis involves the assignment of elements to the characteristic X-ray peaks recognized in the energy dispersive X-ray spectrometry (EDS) spectrum. This function is routinely performed with automatic peak identification (e.g., "AutoPeakID") software embedded in the vendor EDS system. While automatic peak identification is a valuable tool, the careful analyst will always manually identify elements by hand first and only use the automatic peak identification to confirm the manual elemental identification, even at the level of major constituents (mass concentration, $C > 0.1$), but especially for minor ($0.01 \le C \le 0.1$) and trace ($C < 0.1$) constituents. Using automatic peak identification before manual identification tends to lead to a cognitive flaw called confirmation bias - the tendency to interpret data in a way that confirms one's preexisting beliefs or hypotheses.

18.1 Quality Assurance Issues for Qualitative Analysis: EDS Calibration

Before attempting automatic or manual peak identification, it is critical that the EDS system be properly calibrated to ensure that accurate energy values are measured for the characteristic X-ray peaks. Follow the vendor's recommended procedure to rigorously establish the calibration. The calibration procedure typically involves measuring a known material such as copper that provides characteristic X-ray peaks at low photon energy (e.g., Cu L_3-M_5 at 0.928 keV) and at high photon energy (Cu K-L_3 at 8.040 keV). Alternatively, a composite aluminum-copper target (e.g., a copper penny partially wrapped in aluminum foil and continuously scanned so as to excite both Al and Cu) can be used to provide the Al K-L_3 (1.487 keV) as the low energy peak and Cu K-L_3 for the high energy peak. After calibration, peaks occurring within this energy range (e.g., Ti K-L_3 at 4.508 keV and Fe K-L_3 at 6.400 keV) should be measured to confirm linearity. A well-calibrated EDS should produce measured photon energies within ±2.5 eV of the ideal value. Low photon energy peaks below 1 keV photon energy should also be measured, for example, O K (e.g., from MgO) and C K. For some EDS systems, nonlinearity may be encountered in the low photon energy range. ◘ Figure 18.1 shows an EDS spectrum for $CaCO_3$ in which the O K peak at 0.523 keV is found at the correct energy, but the C K peak at 0.282 keV shows a significant deviation below the correct energy due to non-linear response in this range caused by incomplete charge collection.

All calibration spectra should be stored as part of the laboratory Quality Assurance documentation, and the calibration procedure should be performed regularly, preferably weekly and especially whenever the EDS system is powered down and restarted.

18.2 Principles of Qualitative EDS Analysis

The knowledge base needed to accomplish high-confidence peak identification consists of three components: (1) the physics of characteristic X-ray generation and propagation; (2) a complete database of the energies of all critical ionization energies and corresponding characteristic peaks for all elements (except H and He, which do not produce characteristic X-rays); and (3) the artifacts inherent in EDS measurement.

18.2.1 Critical Concepts From the Physics of Characteristic X-ray Generation and Propagation

What factors determine if characteristic peaks are generated and detectable?

Exciting Characteristic X-Rays

A specific characteristic X-ray can only be produced if the incident beam energy, E_0, exceeds the critical ionization energy, E_c, for the atomic shell whose ionization leads to the emission of that characteristic X-ray. This requirement is parameterized as the overvoltage, U_0:

$$U_0 = E_0 / E_c > 1 \tag{18.1}$$

Note that for a particular element, if the beam energy is selected so that $U_0 > 1$ for the K-shell, then for higher atomic number elements with complex atomic shell structures, shells with lower values of E_c will also be ionized; for example, if Cu K-shell X-rays are created, there will also be Cu L-shell X-rays, Au L-family, and Au M-family X-rays, etc.

While $U_0 > 1$ sets the minimum beam energy criterion to generate a particular characteristic X-ray, the relative intensity of that X-ray generated from a thick target (where the thickness exceeds the electron range) depends on the overvoltage and the incident beam current, i_B:

$$I_{ch} \sim i_B \left(U_0 - 1\right)^n \tag{18.2}$$

where the exponent n is approximately 1.5. The X-ray continuum intensity, I_{cm}, that forms the spectral background at all photon energies up to E_0 (the Duane–Hunt limit), arises from the electron *bremsstrahlung* and depends on the photon energy, E_ν, and the beam energy:

$$I_{cm} \sim i_B \left(E_0 - E_v\right) / E_v \tag{18.3a}$$

$$I_{cm} \sim i_B \left(U_0 - 1\right) \qquad \text{for } E_v \sim E_c \tag{18.3b}$$

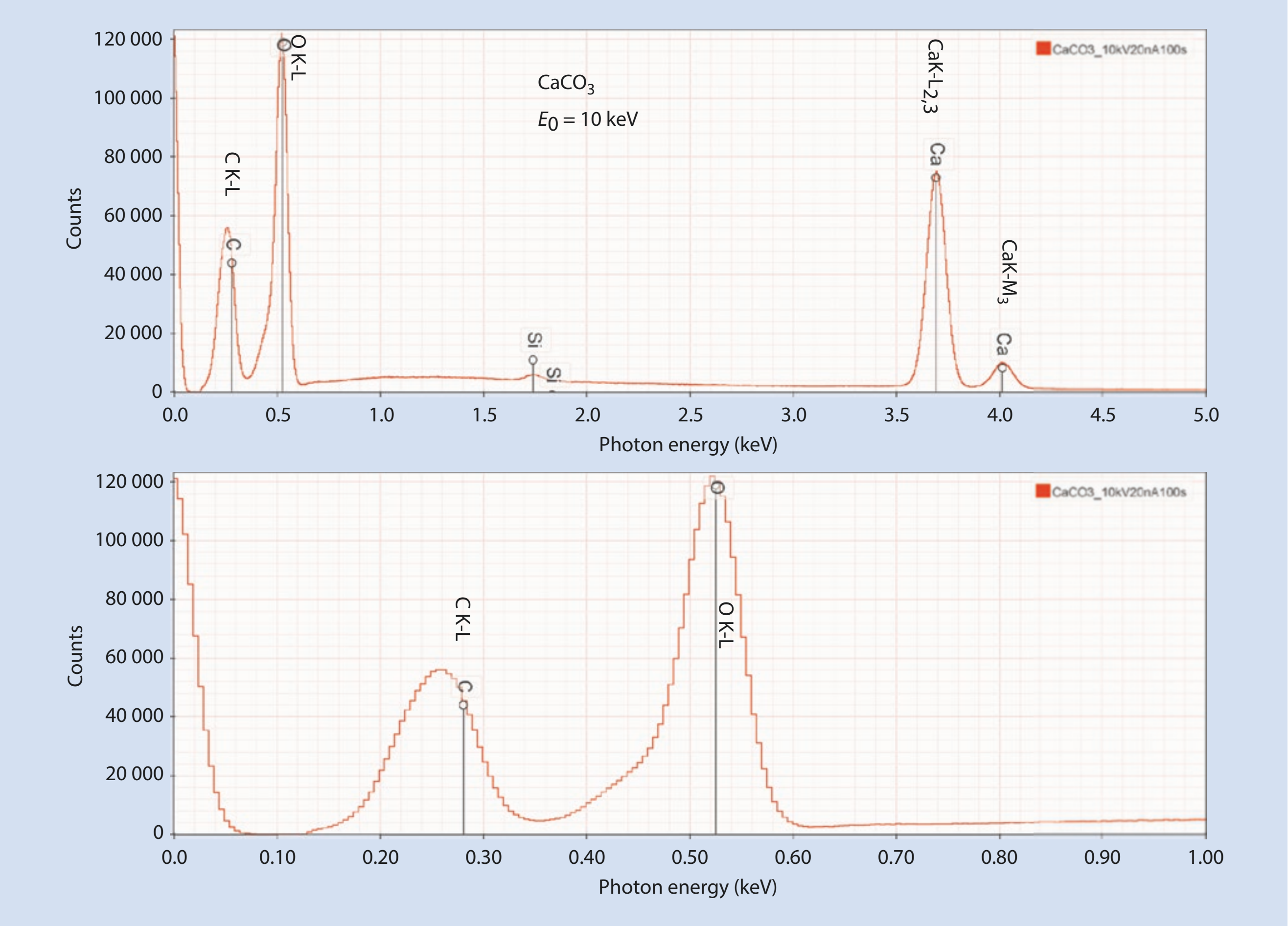

Fig. 18.1 Spectrum of calcium carbonate. Note non-linear behavior at low photon energy, e.g., the C K-shell peak is significantly shifted below the true energy value given by the marker

The characteristic peak to continuum background, P/B, which determines the visibility of peaks above the background, is found as the ratio of equations (18.2) and (18.3b):

$$P/B = I_{\text{ch}} / I_{\text{cm}} \sim (U_0 - 1)^{\text{n}} / (U_0 - 1) = (U_0 - 1)^{\text{n}-1} \tag{18.4}$$

Since the exponent $n \sim 1.5$, in the expression for P/B the value of $n - 1 \sim 0.5$, so that as U_0 is lowered, the P/B decreases dramatically, reducing the visibility of peaks, as shown in Fig. 18.2 for the K-shell peaks of silicon.

Fluorescence Yield

A second factor that affects the detectability of characteristic peaks is the fluorescence yield, the fraction of ionizations that leads to photon emission. The fluorescence yield varies sharply depending on the shells involved, with the fluorescence yields for a particular element generally trending K > L >> M. An example for barium L-shell and M-shell X-rays is shown in Fig. 18.3, where the Ba M-family X-rays are seen to have a much lower P/B than the Ba L-family X-rays, making Ba difficult to identify with high confidence if only the Ba M-family is excited, a condition that will exist for Ba if E_0 is chosen below the 5.25 keV ionization energy for the Ba L_3-shell.

X-ray Absorption

A third factor which can strongly influence the visibility and detection of peaks is absorption of characteristic X-rays as they travel through the specimen and the window and surface layers of the EDS detector. X-ray absorption along a path of length s through the specimen is a non-linear process:

$$I / I_0 = \exp\left[-(\mu / \rho)\rho s\right] \tag{18.5}$$

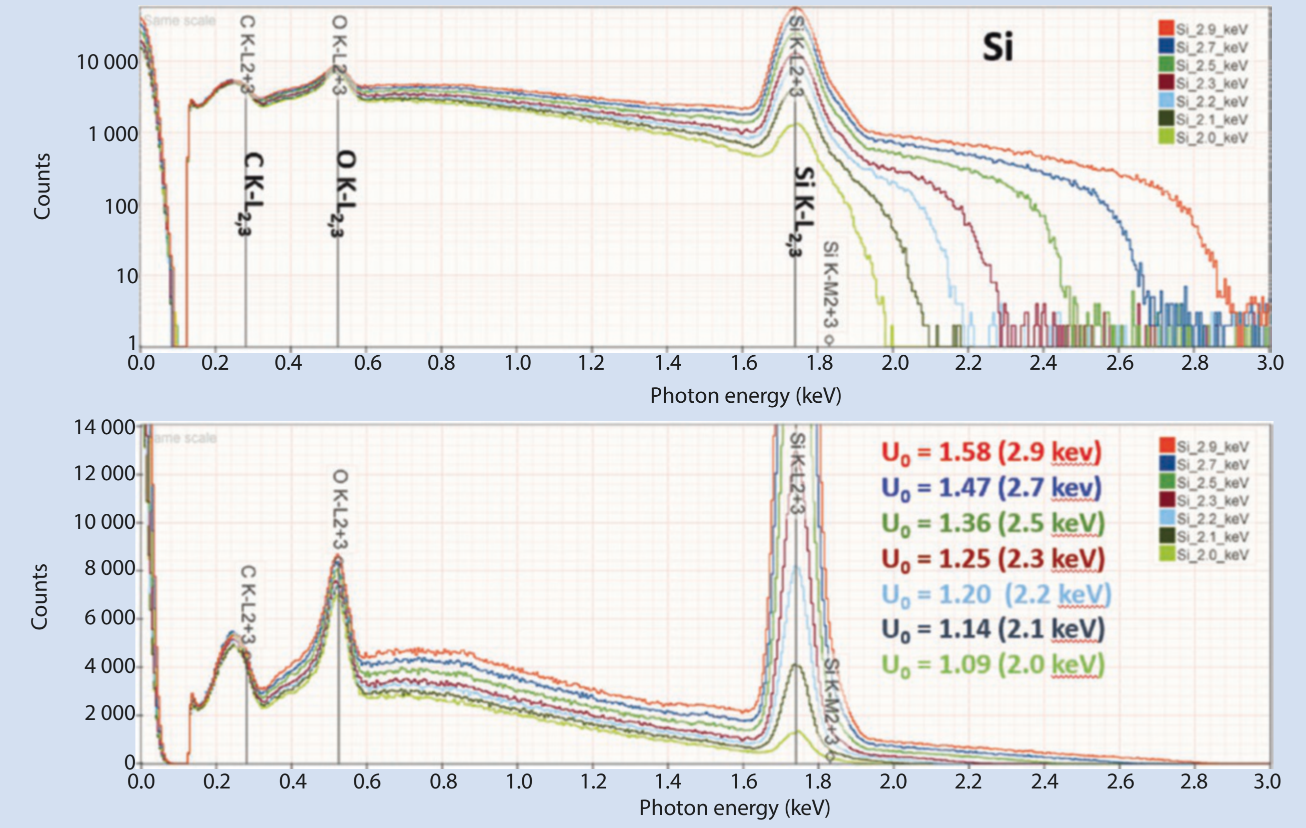

Fig. 18.2 Si at various overvoltages, showing diminishing peak visibility as the excitation decreases

where I_0 is the original intensity and I is the intensity that remains after path s through a material of density ρ having a mass absorption coefficient μ/ρ for the photon energy of interest. The mass absorption coefficient depends strongly on the photon energy and the specific elements that the photons are passing through. Generally, a photon will be strongly absorbed, i.e., there will be a large mass absorption coefficient, if the energy of the photon lies in a range of approximately 1 keV above the critical ionization energy for another element that is present in the analyzed volume. An extreme case is illustrated in Fig. 18.4 for SiC, where at $E_0 = 20$ keV with the spectrum scaled to the Si K-peak, the C K peak is barely visible despite C's making up half of the composition on an atomic basis. Strong absorption of the C K X-ray at 0.282 keV occurs because this energy lies just above the Si L_3 critical ionization energy at 0.110 keV, resulting in an extremely large value for the mass absorption coefficient. (There are also other factors that apply to this case, including the relative fluorescence yields, for which $\omega_{\mathrm{C}} < \omega_{\mathrm{Si}}$, and the relative detector efficiency, $\varepsilon_{\mathrm{C}} < \varepsilon_{\mathrm{Si}}$, as described in the "EDS" module.) Because the absorption path length, s, depends strongly on the electron range, $R_{\text{K-O}}$, which scales approximately as the 1.7 power of the incident beam energy, decreasing the beam energy reduces the absorption path of the C K X-rays, making the C K-peak more prominent relative to the Si K-peak, as shown in Fig. 18.4 for a series of progressively lower beam energies.

The possibility of a high absorption situation for elements that must be measured with a low photon energy requires an analytical strategy such that when analyzing an unknown, the analyst should start at high beam energy, $E_0 \geq 20$ keV, and work down in beam energy. The analyst must be prepared to utilize low beam energies, $E_0 \leq 5$ keV, to evaluate the possibility of high absorption situations, such as those encountered for low atomic number elements ($Z < 10$). For these elements, the only detectable peaks have low photon energies (<1 keV) and are thus subject to high absorption when high incident beam energy is used.

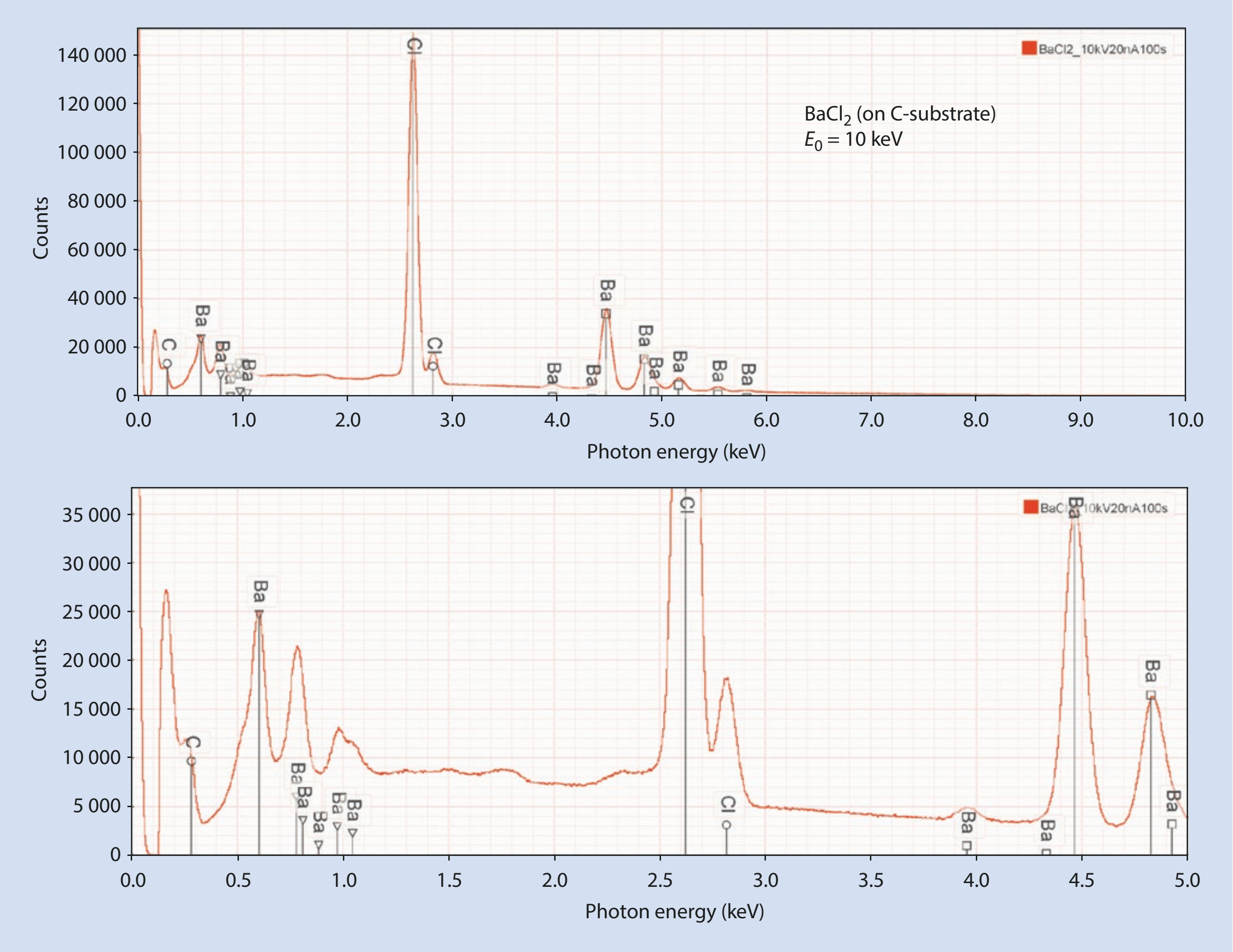

■ **Fig. 18.3** EDS spectrum of BaCl$_2$ showing Ba L-family and Ba M-family peaks

18.2.2 X-Ray Energy Database: Families of X-Rays

The X-ray energy database is typically accessed through EDS software as a display of "KLM" markers showing the position of the peak (and possibly also the corresponding critical ionization energies) and the relative peak heights of the members of each X-ray family, examples of which are seen in ■ Figs. 18.1, 18.2, 18.3, and 18.4. The underlying database must contain such all characteristic X-rays (for ionization energies up to 25 keV) for all elements (excepting H and He which do not produce characteristic X-rays). No elements should be excluded, all X-ray families with photon energies below 30 keV should be included, and no minor X-ray family members should be excluded. As an example, a section of the DTSA-II X-ray energy database that displays the information for gold is presented in ■ Table 18.1. While it is true that many of the closely spaced (in photon energy) and low abundance X-ray peaks cannot be resolved by EDS because of the limited energy resolution, these peaks are nevertheless convolved in the measured spectrum. When a constituent is present at high concentration and is excited with adequate overvoltage, at least some of these low abundance family members will be readily detectable, for example, the L_3-M_1 (Ll) and $M_{4,5}N_{2,3}$ (Mζ) peaks, as shown for Ba in ■ Fig. 18.5 and the $AuM_{4,5}N_{2,3}$, $AuM_1N_{1,3}$ and AuM_2N_4 peaks seen in ■ Fig. 18.6. Note also that the low energy performance of the silicon drift detector (SDD)-EDS is such that the Au N-family peaks are detected.

18.2.3 Artifacts of the EDS Detection Process

The EDS detection process is subject to two principal artifacts that must be properly cataloged to avoid subsequent misidentification.

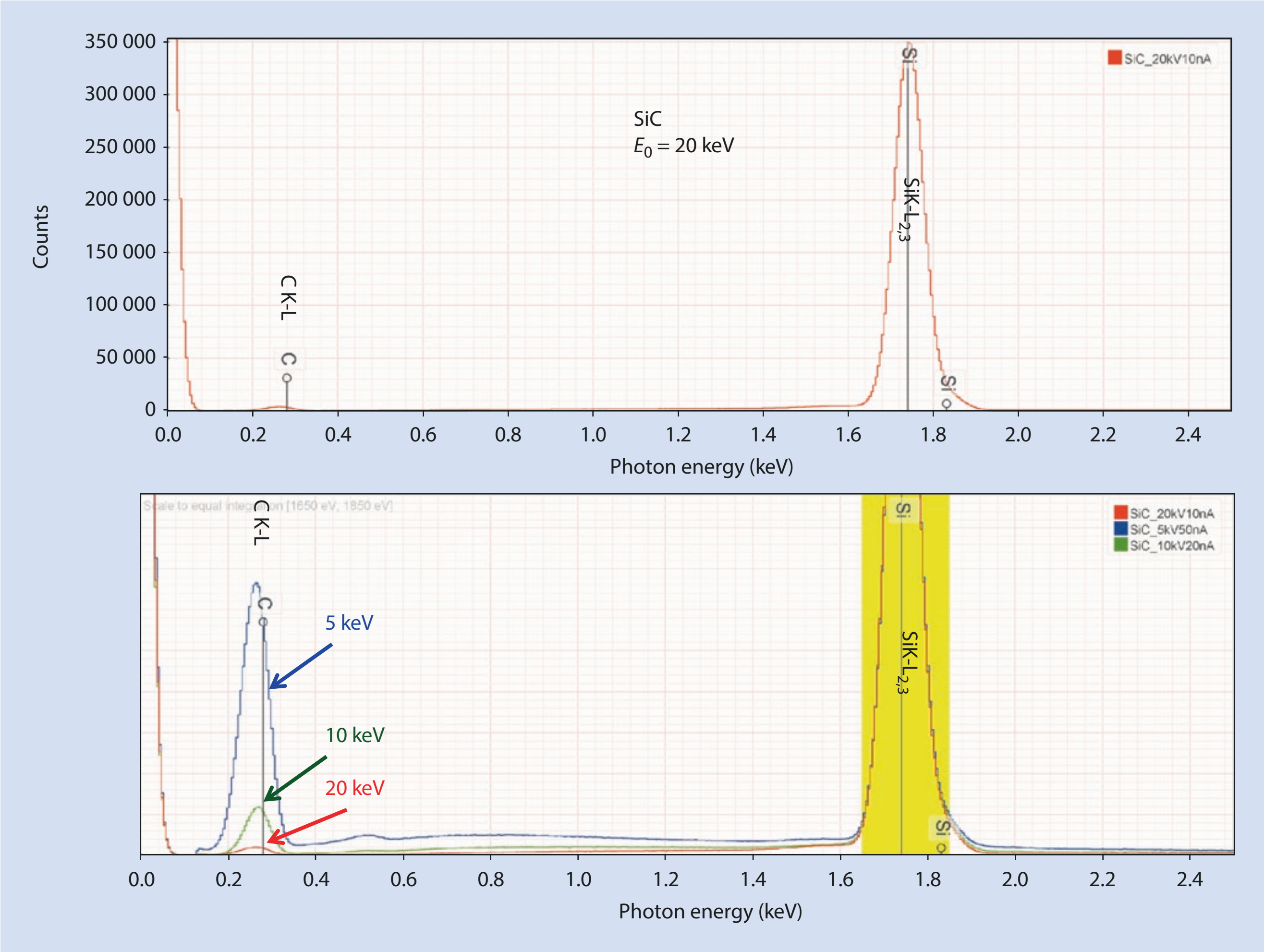

Fig. 18.4 EDS spectra of SiC: (*upper*) at $E_0 = 20$ keV, the C K-L_3 peak is barely visible; (*lower*) as the beam energy is lowered to reduce absorption, the C K-L_3 peak becomes more prominent (all spectra scaled to the Si K-L_3 region.)

Table 18.1 Comprehensive listing of all X-ray transitions for gold (DTSA-II database)

IUPAC	Siegbahn	Weight	Energy (keV)	Wavelength (Å)
Au K-N5	Au Kβ4	0.0000	80.391	0.154226
Au K-N3	Au Kβ2	0.0500	80.1795	0.154633
Au K-M5	Au Kβ5	0.0005	78.5192	0.157903
Au K-M3	Au Kβ1	0.1500	77.9819	0.158991
Au K-M2	Au Kβ3	0.1500	77.5771	0.159821
Au K-L3	Au Kα1	1.0000	68.8062	0.180193
Au K-L2	Au Kα2	0.5000	66.9913	0.185075
Au L1-O4	Au L1O4/L1O5	0.0027	14.3445	0.864333
Au L1-O3	Au Lγ4	0.0062	14.2991	0.867077
Au L1-O2	Au Lγ4p	0.0001	14.2811	0.86817
Au L1-O1	Au L1O1	0.0027	14.245	0.87037

Table 18.1 (continued)

IUPAC	Siegbahn	Weight	Energy (keV)	Wavelength (Å)
Au L1-N5	Au Lγ11	0.0007	14.0189	0.884407
Au L1-N4	Au L1N4	0.0001	14.0008	0.885551
Au L1-N3	Au Lγ3	0.0194	13.8074	0.897955
Au L2-O4	Au Lγ6	0.0109	13.7253	0.903326
Au L1-N2	Au Lγ2	0.0015	13.7091	0.904393
Au L2-O3	Au L2O3	0.0001	13.6799	0.906324
Au L2-O2	Au L2O2	0.0001	13.6619	0.907518
Au L2-N6	Au L*ν*	0.0003	13.6472	0.908495
Au L2-O1	Au Lγ8	0.0007	13.6258	0.909922
Au L1-N1	Au L1N1	0.0001	13.594	0.912051
Au L2-N5	Au L2N5	0.0001	13.3997	0.925276
Au L2-N4	Au Lγ1	0.0841	13.3816	0.926527
Au L2-N3	Au L2N3	0.0027	13.1882	0.940115
Au L2-N2	Au L2N2	0.0001	13.0899	0.947174
Au L2-N1	Au Lγ5	0.0035	12.9748	0.955577
Au L1-M5	Au Lβ9	0.0004	12.1471	1.02069
Au L1-M4	Au Lβ10	0.0054	12.0617	1.02792
Au L3-P1	Au L3P1	0.0001	11.935	1.03883
Au L3-O4	Au Lβ5	0.0438	11.9104	1.04097
Au L3-O2	Au L3O2	0.0001	11.847	1.04655
Au L3-N6	Au Lu	0.0009	11.8323	1.04785
Au L3-O1	Au Lβ7	0.0004	11.8109	1.04974
Au L1-M3	Au Lβ3	0.0690	11.6098	1.06793
Au L3-N5	Au Lβ2	0.2195	11.5848	1.07023
Au L3-N4	Au Lβ15	0.0000	11.5667	1.07191
Au L2-M5	Au L2M5	0.0001	11.5279	1.07551
Au L2-M4	Au Lβ1	0.4015	11.4425	1.08354
Au L3-N3	Au L3N3	0.0001	11.3733	1.09013
Au L3-N2	Au L3N2	0.0001	11.275	1.09964
Au L1-M2	Au Lβ4	0.0594	11.205	1.10651
Au L3-N1	Au Lβ6	0.0140	11.1599	1.11098
Au L2-M3	Au Lβ17	0.0005	10.9906	1.12809
Au L1-M1	Au L1M1	0.0001	10.9279	1.13457
Au L2-M2	Au L2M2	0.0001	10.5858	1.17123
Au L2-M1	Au Lη	0.0138	10.3087	1.20271
Au L3-M5	Au Lα1	1.0000	9.713	1.27648
Au L3-M4	Au Lα2	0.1139	9.6276	1.2878

(continued)

Table 18.1 (continued)

IUPAC	Siegbahn	Weight	Energy (keV)	Wavelength (Å)
Au L3-M3	Au Ls	0.0001	9.1757	1.35122
Au L3-M2	Au Lt	0.0012	8.7709	1.41359
Au L3-M1	Au Lℓ	0.0562	8.4938	1.4597
Au M1-N3	Au M1N3	0.0000	2.8795	4.30575
Au M2-N4	Au M2N4	0.0290	2.7958	4.43466
Au M3-O5	Au M3O5	0.0100	2.73621	4.53124
Au M3-O4	Au M3O4	0.0050	2.73469	4.53375
Au M3-O1	Au M3O1	0.0027	2.6352	4.70493
Au M3-N5	Au Mγ	0.0851	2.4091	5.14649
Au M3-N4	Au M3N4	0.0100	2.391	5.18545
Au M2-N1	Au M2N1	0.0029	2.389	5.18979
Au M4-O2	Au M4O2	0.0010	2.2194	5.58638
Au M4-N6	Au Mβ	0.5944	2.2047	5.62363
Au M5-O3	Au M5O3	0.0001	2.152	5.76135
Au M5-N7	Au Mα1	1.0000	2.1229	5.84032
Au M5-N6	Au Mα2	1.0000	2.1193	5.85024
Au M3-N1	Au M3N1	0.0290	1.9842	6.24857
Au M4-N3	Au M4N3	0.0001	1.7457	7.10226
Au M5-N3	Au Mζ1	0.0134	1.6603	7.46758
Au M4-N2	Au Mζ2	0.0451	1.6474	7.52605
Au N4-N6	Au N4N6	1.0000	0.2656	46.6808
Au N5-N6	Au N5N6/N5N7	1.0000	0.2475	50.0946

Si Escape Peak

The Si escape peak results when a Si K–L_3 X-ray ($E = 1.740$ keV), which is created following the photoionization of a silicon atom and is usually reabsorbed within the detector volume, escapes. This results in an energy loss of 1.740 keV from the parent X-ray, creating a "silicon escape peak," as shown in Fig. 18.7 (upper spectrum) for the titanium K-family X-rays. Escape peaks can only be created for parent photon energies above 1.740 keV and are formed at a fixed fraction of the parent peak, with that fraction rapidly decreasing as the parent X-ray energy increases above 1.740 keV. For parent peaks with photon energies above 6 keV, escape peaks are so small that they are difficult to detect. Escape peaks can occur from any parent peak, but as a practical matter only the major members of a family are likely to produce detectable escape peaks. Note that in the example shown for the titanium K-family in Fig. 18.7, the escape peaks for Ti K-$L_{2,3}$ and Ti K-$M_{2,3}$ are both detected because of the high count spectrum. The EDS system should mark all possible escape peaks and not subsequently misidentify them as other elements. For example, if not properly assigned, the escape peak for Ti K-$L_{2,3}$ could be mistaken for Cl K-$L_{2,3}$. Note that some vendor software removes the escape peaks in the final processed spectrum that is displayed to the user, as shown in Fig. 18.7 (lower spectrum).

Coincidence Peaks

Although the EDS spectrum may appear to an observer to be collected simultaneously at all photon energies, in reality only one photon can be measured at a time. Because X-rays are created randomly in time, as the rate of production (input count rate) increases, the possibility of two photons entering the detector and creating an artifact coincidence event increases in probability. An inspection function continuously monitors the detector to reject such events, but at

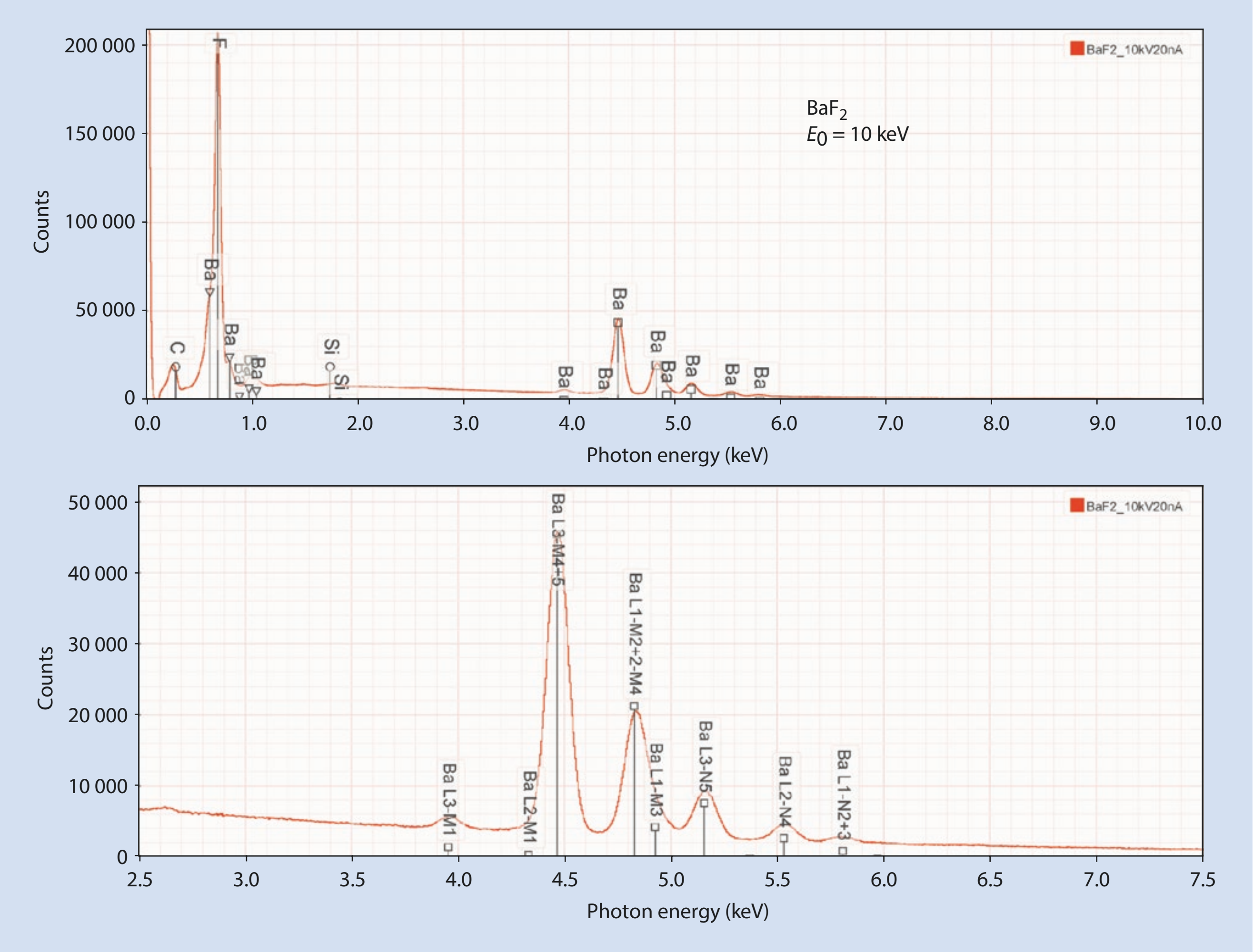

Fig. 18.5 EDS spectrum of BaF$_2$ excited with a beam energy of 10 keV

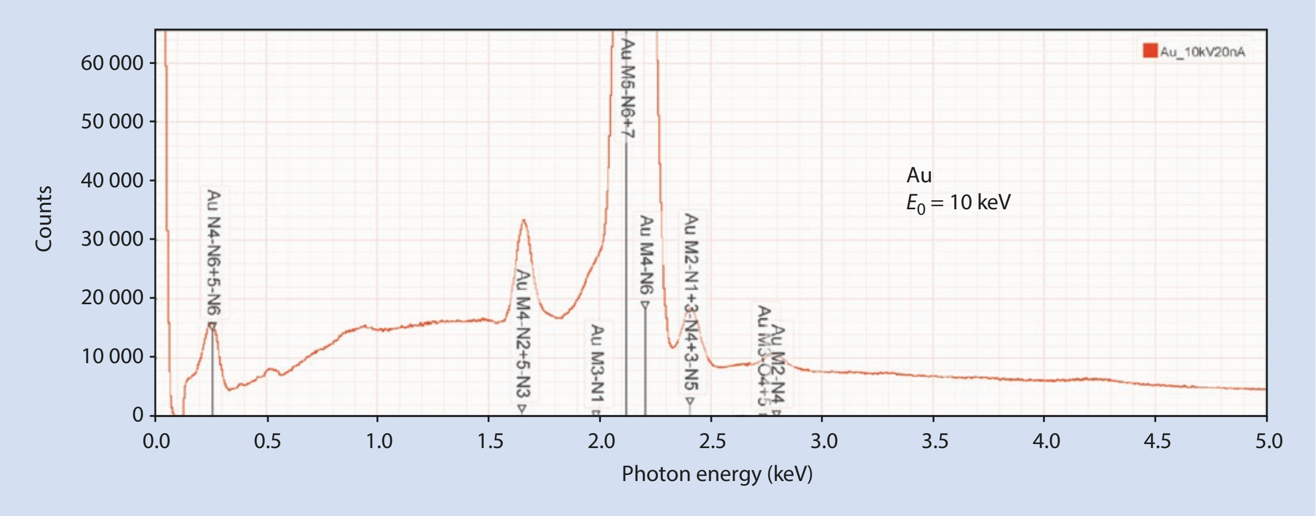

Fig. 18.6 EDS spectrum of Au excited with a beam energy of 10 keV

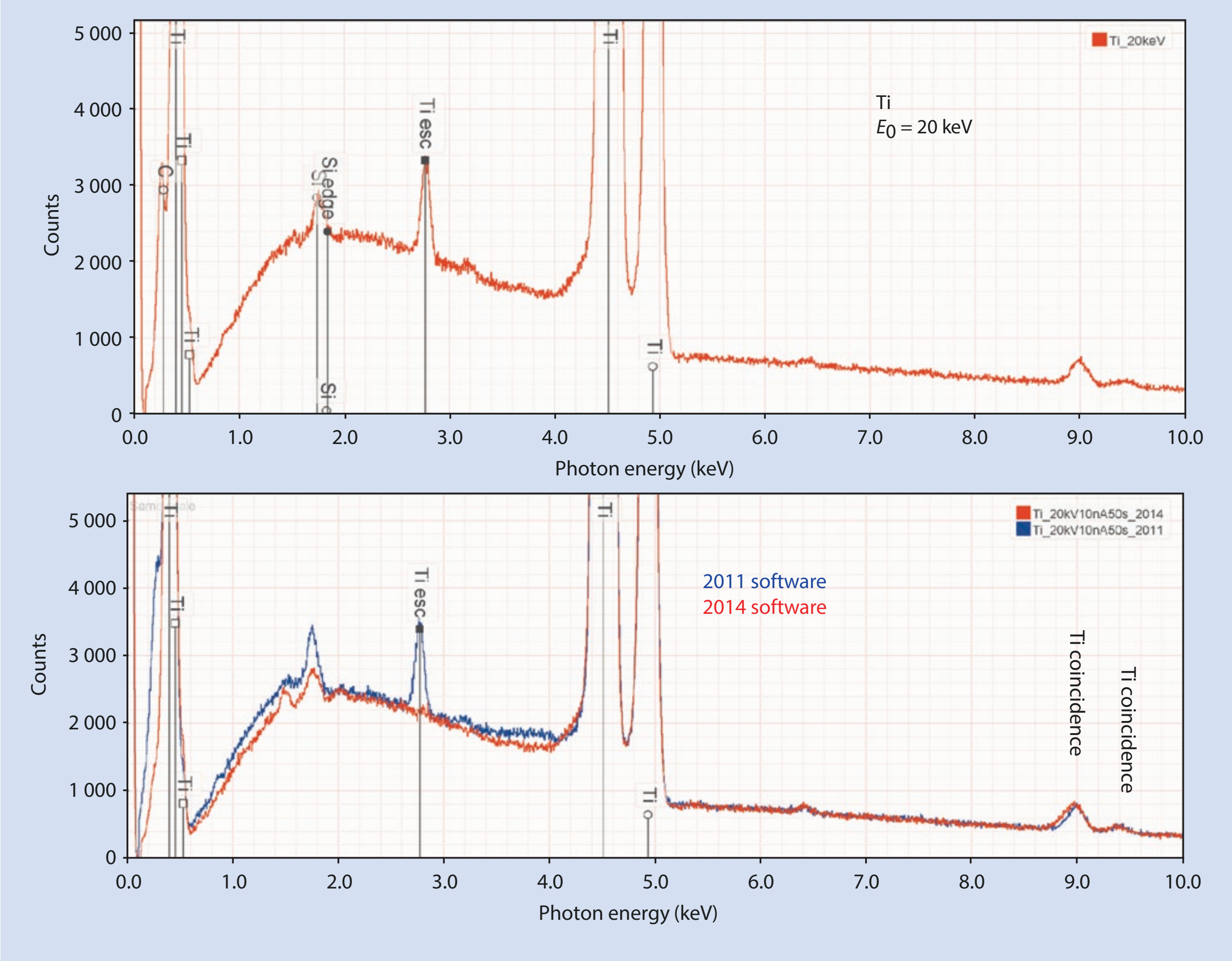

■ **Fig. 18.7** EDS spectrum of titanium recorded at $E_0 = 20$ keV and a dead-time of 11 %

sufficiently high input count rates its finite time resolution will be overwhelmed and coincidence events will begin to populate the spectrum. This phenomenon is illustrated in ■ Fig. 18.7 for pure Ti, where coincidence peaks are seen for Ti K-L$_{2,3}$ + Ti K-L$_{2,3}$ and Ti K-L$_{2,3}$ + Ti K-M$_{2,3}$. The height of a coincidence peak relative to the parent peak depends on the arrival rate of X-rays at the detector, and thus upon the dead-time. Even at low dead-time coincidence events are likely to be observed for highly excited, low photon energy peaks such as Al and Si in pure element or high concentration targets, as shown for Si in ■ Fig. 18.8 at 12 % dead-time and in ■ Fig. 18.9 at 1 % dead-time. Operating at low dead-time can reduce the height of the coincidence peak relative to the parent peak, but coincidence can never entirely be eliminated by reducing the input count rate. For complex compositions, a wide array of coincidence peaks involving many combinations of highly excited peaks can be encountered, as shown in ■ Fig. 18.10. As the dead-time increases, numerous coincidence peaks are observed, several of which could be misidentified as elements present as trace to minor constituents. At the highest dead-times, the coincidence peaks are seen to occupy much of the useful spectral energy range where legitimate minor and trace constituents might be measured. Coincidence can involve any two photons of any energies, but the noticeable effects in EDS spectra consist of two characteristic peak photons that originate from major constituents that are highly excited, for exmple, A + A, A + B, B + B, an so on. Since coincidence depends on the arrival rate of photons, the analyst can exert some control by operating at low dead-time (10 % or less) to minimize but not eliminate the effect. Some vendor EDS systems use statistical models of coincidence to post process the spectrum, removing the coincidence events and restoring the events to their proper parent peaks.

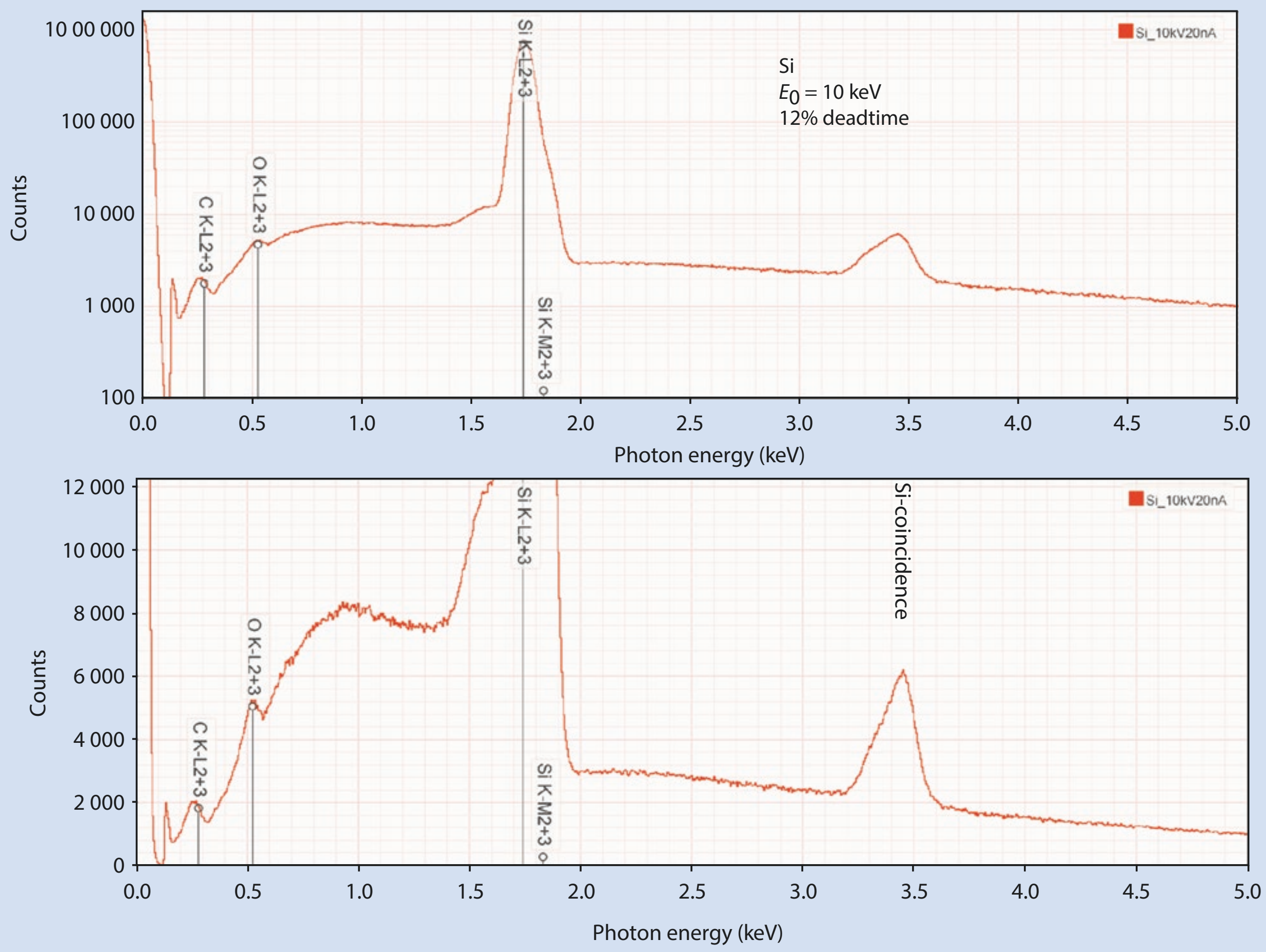

◘ **Fig. 18.8** EDS spectrum of silicon at a dead-time of 12 %

18.3 Performing Manual Qualitative Analysis

18.3.1 Why Are Skills in Manual Qualitative Analysis Important?

The automatic peak identification function supplied in all vendor software is a powerful and useful tool, but it should only be used to confirm manual identifications rather than vice versa. Studies have shown that incorrect peak assignments occur with vendor software in a few percent of analyses even for major constituents ($C > 0.1$ mass fraction, 10 weight percent) that produce prominent spectral peaks (Newbury 2005). ◘ Table 18.2 lists groups of elements for which incorrect peak assignments have been observed in vendor software from different sources. Extensive observations suggest that peak misidentifications occur for major constituents in several percent of qualitative analyses of major constituents. The problem of incorrect assignments becomes even more significant for minor and trace constituents that produce peaks that inevitably occur at low peak-to-background and for which it may be difficult to recognize more than one characteristic peak (Newbury 2009). The frequency of incorrect peak assignments for minor and trace constituents can be 10 % or more, with both false positives (incorrect peak assignments) and false negatives (legitimate peaks ignored). For operation at low beam energy where the incident beam energy restricts the atomic shells which can be ionized to produce X-rays, peak identification is even more problematic at all concentration levels (Newbury 2007).

For minor and trace constituents, incorrect elemental identifications arise from incomplete identification of minor family members of X-ray families actually associated with previously identified major constituents, as well as artifact

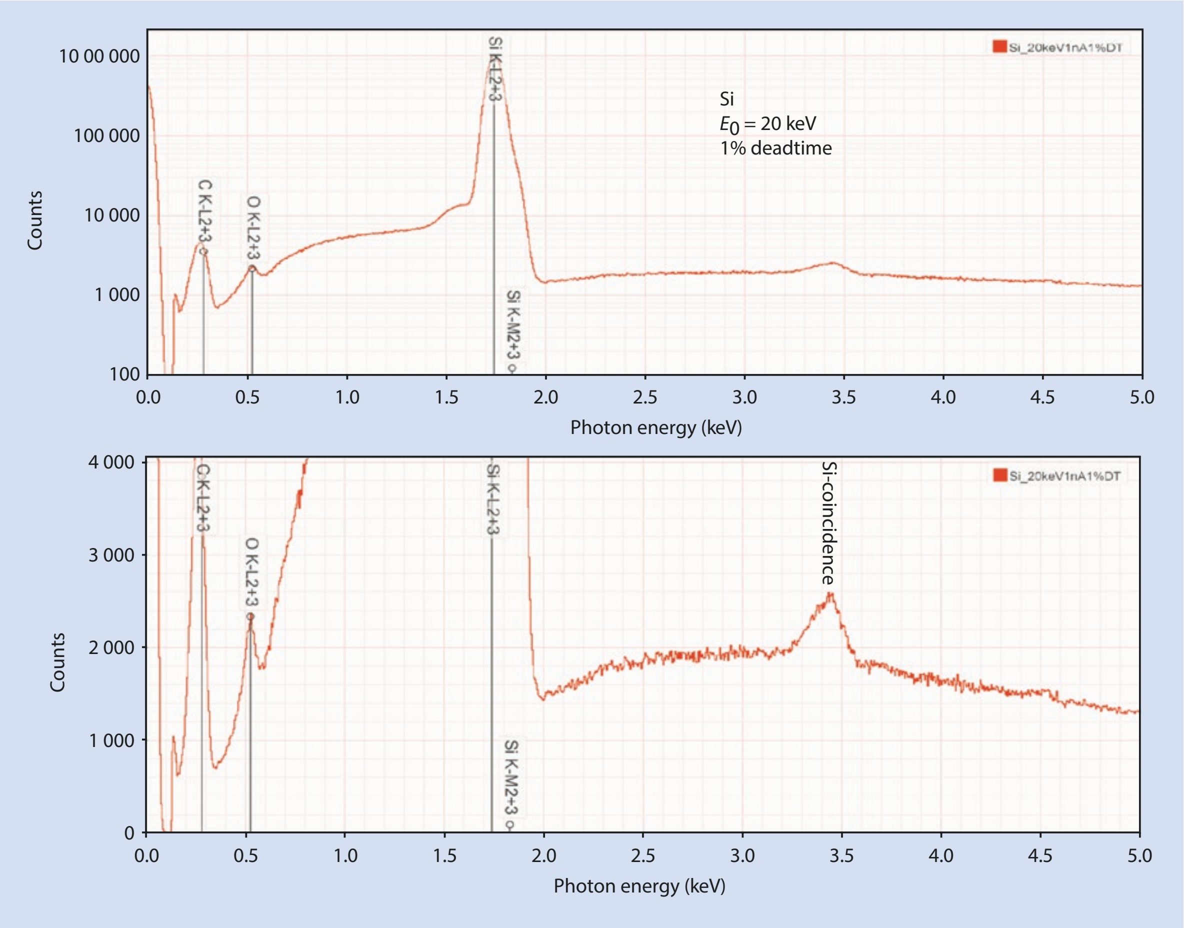

Fig. 18.9 EDS Spectrum of silicon at a dead-time of 1 %

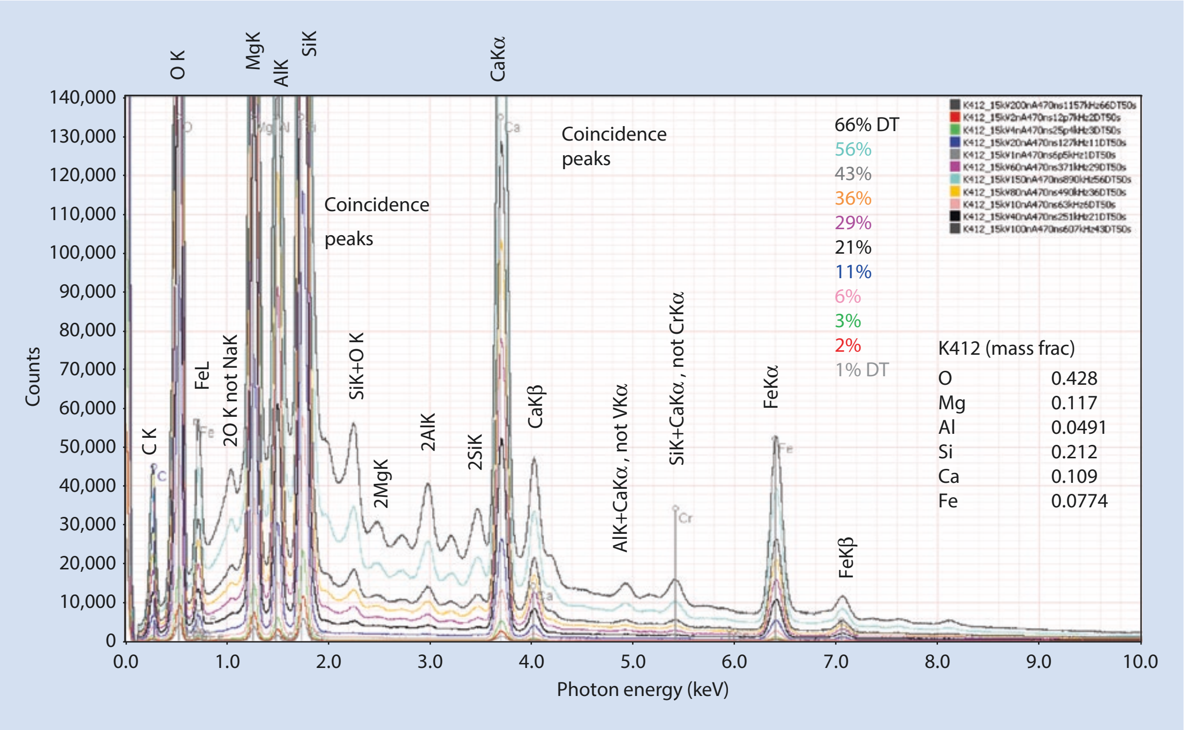

Fig. 18.10 EDS spectra of NIST glass K412 over a range of dead-times from 1 % to 66 %

Table 18.2 Characteristic X-ray peaks vulnerable to misidentification

Energy range	Elements, peaks, and photon energies
0.390–0.395 keV	N K-L_3 (0.392); Sc L_3-$M_{4,5}$ (0.395)
0.510–0.525 keV	O K-L_3 (0.523); V L_3-$M_{4,5}$ (0.511)
0.670–0.710 keV	F K-L_3 (0.677); Fe L_3-$M_{4,5}$ (0.705) (0.677); Fe L_3-$M_{4,5}$ (0.705)
0.845–0.855 keV	Ne K-L_3 (0.848); Ni L_3-$M_{4,5}$ (0.851)
1.00–1.05 keV	Na K-$L_{2,3}$ (1.041); Zn L_3-$M_{4,5}$ (1.012); Pm M_5-$N_{6,7}$ (1.032)
1.20–1.30 keV	Mg K-$L_{2,3}$ (1.253); As L_3-$M_{4,5}$ (1.282); Tb M_5-$N_{6,7}$ (1.246)
1.45–1.55 keV	Al K-$L_{2,3}$ (1.487); Br L_3-$M_{4,5}$ (1.480); Yb M_5-$N_{6,7}$ (1.521)
1.70–1.80 keV	Si K-$L_{2,3}$ (1.740); Ta M_5-$N_{6,7}$ (1.709); W M_5-$N_{6,7}$ (1.774)
2.00–2.05 keV	P K-$L_{2,3}$ (2.013); Zr L_3-$M_{4,5}$ (2.042); Pt M_5-$N_{6,7}$ (2.048)
2.10–2.20 keV	Nb L_3-$M_{4,5}$ (2.166); Au M_5-$N_{6,7}$ (2.120); Hg M_5-$N_{6,7}$ (2.191)
2.28–2.35 keV	S K-$L_{2,3}$ (2.307); Mo L_3-$M_{4,5}$ (2.293); Pb M_5-$N_{6,7}$ (2.342)
2.40–2.45 keV	Tc L_3-$M_{4,5}$ (2.424); Pb M_4-N_6 (2.443); Bi M_5-$N_{6,7}$ (2.419)
2.60–2.70 keV	Cl K-$L_{2,3}$ (2.621); Rh L_3-$M_{4,5}$ (2.696)
2.95–3.00 keV	Ar K-$L_{2,3}$ (2.956); Ag L_3-$M_{4,5}$ (2.983); Th M_5-$N_{6,7}$ (2.996)
3.10–3.20 keV	Cd L_3-$M_{4,5}$ (3.132); U M_5-$N_{6,7}$ (3.170)
3.25–3.35 keV	K K-$L_{2,3}$ (3.312); In L_3-$M_{4,5}$ (3.285); U M_4-N_6 (3.336)
4.45–4.55 keV	Ti K-$L_{2,3}$ (4.510); Ba L_3-$M_{4,5}$ (4.467)
4.90–5.00 keV	Ti K-M_3 (4.931); V K-$L_{2,3}$ (4.949)

peaks that arise from the silicon escape peak and from coincidence peaks. A particularly insidious problem occurs when automatic peak identification software delivers identifications of peaks with low peak-to-background too early in the EDS accumulation before adequate counts have been recorded. Statistical fluctuations in the continuum background create "false peaks" that may appear to correspond to minor or trace constituents. This problem can be recognized when an apparent peak identification solution for these low level peaks subsequently changes as more counts are accumulated. The danger is that the analyst may choose to stop the accumulation prematurely and be misled by the low level "peaks" that do not actually exist.

When the analyst must operate only at low beam energy ($E_0 \leq 5$ keV), the peak misidentification problem is exacerbated by the loss of the higher photon energies where X-ray family members are more widely spread and more easily identified, as well as the confidence-increasing redundancy provided by having K-L and L-M family pairs for identification of intermediate and high atomic number elements (Newbury 2009).

Even well-implemented automatic peak identification software is likely to ignore peaks with low peak-to-background that may correspond to trace constituents because the likelihood of a mistake becomes so large. Thus, if it is important to the analyst to identify the presence of a trace element (s) with a high degree of confidence, manual peak identification will be necessary.

18.3.2 Performing Manual Qualitative Analysis: Choosing the Instrument Operating Conditions

Beam Energy

Equation 18.1 reveals that one selection of the beam energy may not be sufficient to solve a particular problem, and the analyst must be prepared to explore a range of beam energies to access desired atomic shells. The peak height relative to the spectral background increases rapidly as U_0 is increased, enabling better detection of the characteristic peak (s). Having adequate overvoltage is especially important as the concentration of an element decreases from major to minor to trace. As a general rule, it is desirable to have $U_0 > 2$ for the analyzed shells of all elements that occur in a particular analysis. For initial surveying of an unknown specimen, it is useful to select a beam energy of 20 keV or higher to provide an overvoltage of at least 2 for ionization edges up to 10 keV. Elements with intermediate atomic numbers (e.g., 22, Ti $\leq Z \leq$ 42, Mo) and high atomic number (e.g., $Z \geq 56$, Ba) elements have complex atomic shell structures that produce two families of detectable characteristic X-rays (with 20 keV $\leq E_0 \leq$ 30 keV), for example, the Cu K-family and L-family; the Au L-family and M-family. A second advantage of selecting the beam energy to excite the higher energy X-ray family for an element is that it enables a high confidence identification since the peaks that form the family are more widely separated in photon energy and thus more likely to be resolved with EDS. Note that the physics of X-ray generation requires that all members of the X-ray family of a tentative elemental assignment must be present. Identifying all family members in the correct relative intensity ratios gives high confidence that the element assignment is correct as well as avoiding subsequent misidentification of these minor family members.

Choosing the EDS Resolution (Detector Time Constant)

EDS systems provide two or more choices for the detector time constant. The user has a choice of a short detector time constant that gives higher throughput (photons recorded per unit time) at the expense of poorer peak resolution or a long time constant that improves the resolution at the cost of throughput. The analyst thus has a critical choice to make: more counts per unit time or better resolution. Statham (1995) analyzed these throughput-resolution trade-offs with respect to various analytical situations and concluded that a strategy that emphasizes maximizing the number of X-ray counts rather than resolution produces the most robust results.

Choosing the Count Rate (Detector Dead-Time)

A closely related consideration is the problem of pulse coincidence creating artifact peaks, which are reduced (but not eliminated) by using lower dead-time. Note that a specific level of dead-time, for example, 10 %, corresponds to a higher throughput when a shorter time constant is chosen. With the beam energy and detector time constant selected, the rate at which X-rays arrive at the EDS and subsequent output depends on two factors: (1) the detector solid angle and (2) the beam current. If the EDS detector is movable relative to the specimen, the specimen-to-detector distance should be chosen in a consistent fashion to enable subsequent return to the same operating conditions for robust standards-based quantitative analysis. A typical choice is to move the detector as close to the specimen as possible to maximize the detector solid angle, $\Omega = A/r^2$, by minimizing r, the detector-to-specimen distance, where A is the active area of the detector. Always ensure that any possible stage motions will not cause the specimen to strike the EDS. With the EDS solid angle fixed, the input count rate will then be controlled by the beam current. A useful strategy is to choose a beam current that creates an EDS dead-time of approximately 10 % on a highly excited characteristic X-ray, such as Al K-$L_{2,3}$ from pure aluminum. To establish dose-corrected standards-based quantitative analysis, this same detector solid angle and beam current should be used for all measurements. It is often desirable to maximize the recorded counts per unit of real (clock) time. Higher beam current leading to higher dead-time, for example, 30–40 %, can be utilized, but the spectrum is likely to have coincidence peaks like those shown in ◘ Fig. 18.10, which can greatly complicate the recognition and measurement of the peaks of minor and trace constituents. Note that some vendor software systems effectively block coincidence peaks or else remove them from the spectrum by post-processing with a stochastic model that predicts coincidence peaks based on the parent peak count rates.

Obtaining Adequate Counts

The analyst must accumulate adequate X-ray counts to distinguish a peak against the random fluctuations of the background (X-ray continuum). While it is relatively easy to record sufficient counts to recognize the principal peak for a major constituent, detection of the minor family member (s) to increase confidence in the elemental assignment may require recording a substantially greater total count. For minor or trace constituents, an even greater dose is likely to be required just to detect the principal family members, and to obtain minor family members to increase confidence in an elemental identification will require a dose greater by another factor of ten or more. A peak is considered *detectable* if it satisfies the following criterion (Currie 1968):

$$n_P > 3 n_B^{1/2} \quad (18.6)$$

where n_P is the number of peak counts and n_B is the number of background counts under the peak. Note that "detectable" does not imply optimally measureable, for example, obtaining accurate peak energy. While Eq. 18.6 defines the minimum counts to detect a peak, accurate measurement of the peak position to identify the peak may require higher counts. The effect of increasing the total spectral intensity to "develop" low relative intensity peaks from trace constituents is shown in ◘ Fig. 18.11.

▪▪ Golden Rule

If it is difficult to recognize a peak above fluctuations in the background, accumulate more counts. Patience is a virtue!

18.4 Identifying the Peaks

After a suitable spectrum has been accumulated, the analyst can proceed to perform manual qualitative analysis.

18.4.1 Employ the Available Software Tools

Manual qualitative analysis is performed using the support of available software tools such as KLM markers that show the energy positions and relative heights of X-ray family members to assign peaks recognized in the spectrum to specific elements. Before using this important software tool, the user

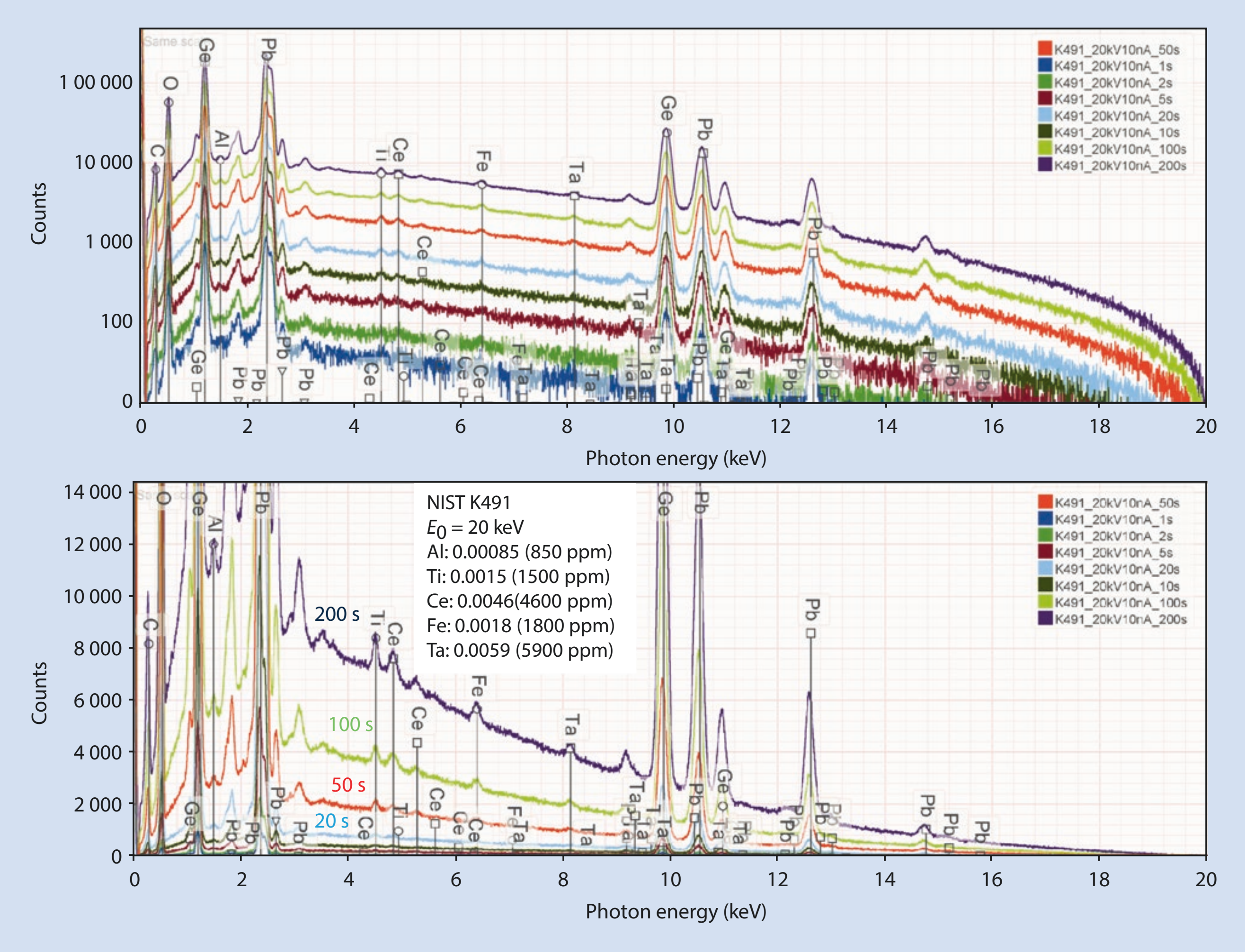

Fig. 18.11 Detection of trace constituent peaks in NIST microanalysis glass K491 as the dose is increased. Integrated spectrum counts: 1 s = 0.14 million; 2 s = 0.28 million; 5 s = 0.70 million; 10 s = 1.4 million; 20 s = 2.8 million; 50 s = 7.1 million; 100 s = 14.3 million; 200 s = 28.5 million

should confirm that all elements in the periodic table are enabled and all X-ray family members are shown in the KLM markers.

As each element is tentatively identified from its major family peak, a systematic search must then be made to locate all possible peaks that *must* be associated with that element: (1) all minor family members; (2) a second X-ray family at lower energy (e.g., K and L or L and M), and for the highest atomic number elements, the N-family can also be observed, as shown in Fig. 18.6; and (3) any associated EDS artifact peaks (escape peaks and coincidence peaks). This careful inspection regimen and meticulous bookkeeping raises the confidence in the tentative assignment. Properly assigning the minor family members and the artifact peaks to the proper element will diminish the possibility of subsequent incorrect assignment of those peaks to other constituents that might appear to be present at minor or trace levels.

It can be helpful to think of qualitative analysis as the process of eliminating those elements which cannot possibly be present rather than the process of including those that definitely are present. It isn't the natural perspective and it takes more thought and effort but it is much less prone to errors of omission.

Imagine that you are at a zoo. You have a list of 20 animals of various sizes and shapes and you are asked to answer the question, what animals in this list *could possibly* be in this cage. You look around and see a rhinoceros laying down near the back of the cage and no other animal. You might be tempted to say that the only animal that could possibly be in the cage is the one you see – the rhinoceros. However, the list also contains snakes, mice, fish and elephants. You can rule out elephants because they are too big to hide behind a rhino. You can rule out fish because the environment is inappropriate. You can't rule out the possibility that a mouse or snake is in the cage hidden behind the rhino. It is only by eliminating those animals that are too large (elephant) or can't survive (fish) behind the rhino that you can come to the full list of animals that could potentially be present in the cage – the rhino and any animals which could be hiding behind the rhino. If you want to be certain that you haven't missed an animal that could *possibly* be present in the cage, the process of culling animals that couldn't possibly be present is far more robust than the process of including animals that definitely are present.

Spectra are similar. Not only is it possible that the obvious elements are present but also those that could be hidden by the ones that are readily identified. Fortunately, there is a tool to help us to see through spectra and expose the hidden components – the residual spectrum. The residual spectrum is the intensity that remains in each channel after peak fitting has been performed for the specified elements. It is like being able to ask the rhino to move and then being able to see what is hidden behind – maybe a mouse or a snake or maybe nothing. An example of the utility of the residual spectrum is shown in Figure 20.8.

18.4.2 Identifying the Peaks: Major Constituents

Start with peaks located in the higher photon energy (>4 keV) region of the spectrum and work downward in energy, even if there are higher peaks in the lower photon energy region (<4 keV). The logic for this strategy is that K-shell and L-shell characteristic X-rays above 4 keV are produced in families that provide two or more peaks with distinctive relative abundances for which the energy resolution of EDS is sufficient to easily separate these peaks. Having two or more peaks to identify greatly increases the confidence with which an elemental identification can be made, enabling the analyst to achieve an unambiguous result. For each peak that is recognized, first test whether its energy corresponds closely to a particular K-L_3 (Kα) peak. The physics of X-ray generation demands that the corresponding K-M_3 (Kβ) peak must also be present in roughly a 10:1 ratio. If K-family peaks do not match the peak in question, examine L-family possibilities, noting that three or more L-peaks are likely to be detectable: L_3–$M_{4,5}$ (Lα), L_2-M_4 (Lβ), and L_2-N_4 (Lγ). Locate and mark all minor family members such as L_3-M_1 (Ll). Locate and mark the escape peaks, if any, associated with the major family members. Locate and mark, if any, the coincidence peaks associated with the major family members, which may be located at very high energy, for example, as shown for Cu K-L_3 coincidence in ▣ Fig. 18.12.

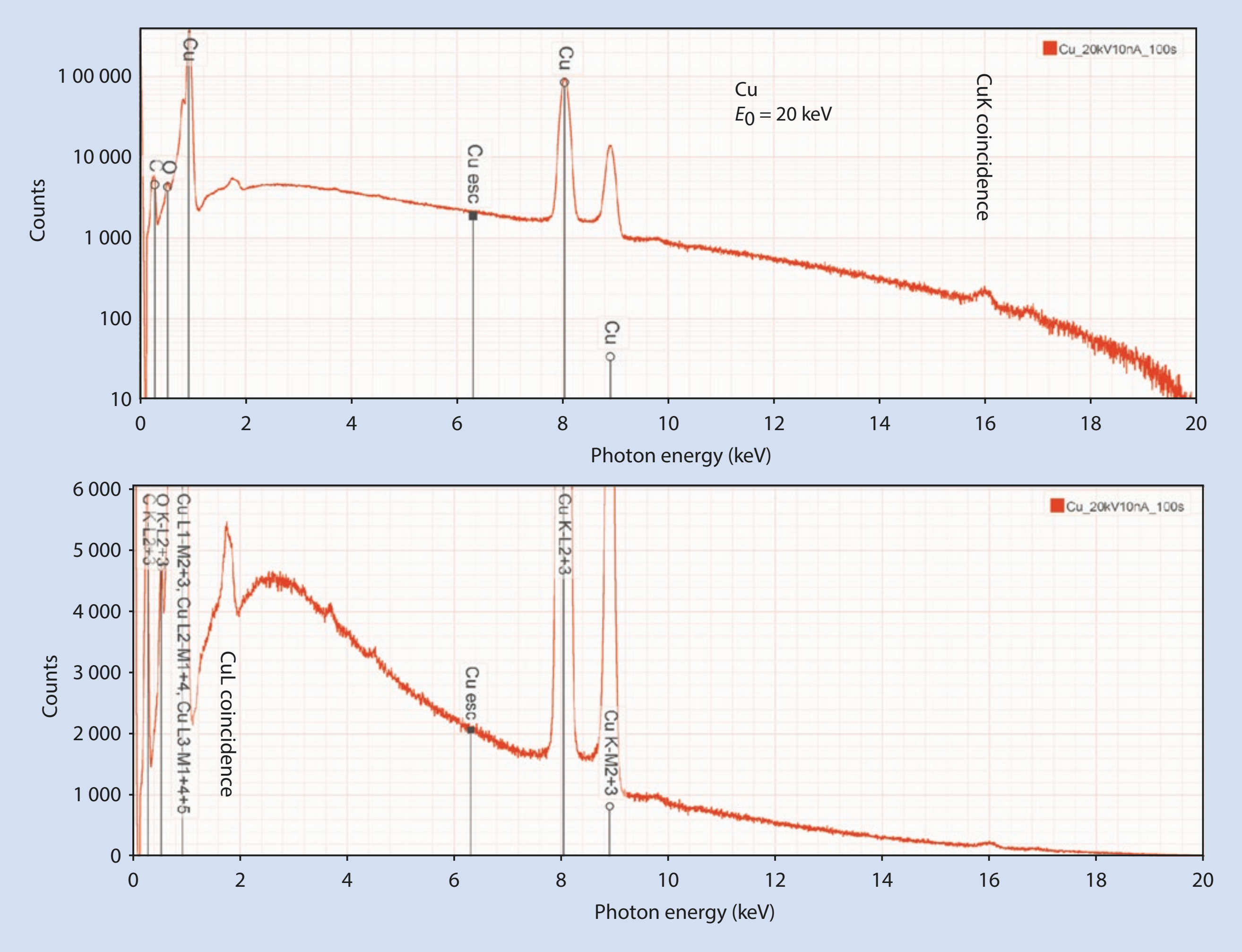

▣ **Fig. 18.12** EDS spectrum of Cu at $E_0 = 20$ keV showing a coincidence peak for CuK-L_3 at 16.08 keV

18.4.3 Lower Photon Energy Region

As major spectral peaks located at lower photon energy (<4 keV) are considered, the energy separation diminishes and the relative peak heights decrease for the members of each X-ray family. EDS is no longer able to resolve these peaks, leading to a situation where only one peak is available for identification for K-family X-rays below 2 keV in energy. The K-L_3 peak appears symmetric since the K-M_3 peak has low relative intensity, as shown for Al K-L_3 in ◘ Fig. 18.13a. For L- and M-family X-rays in the low photon energy range, the composite peak appears asymmetric. As shown for Br in ◘ Fig. 18.13b, the major peaks L_3-M_5(Lα) and L_2-M_4(Lβ) occur with a ratio of approximately 2:1 and the low abundance but separated L_3-M_1 (Ll) and L2-M1 (Lη) can also aid in the identification providing the spectrum contains adequate counts. Similarly, the M_5-$N_{6,7}$(Mα) and M_4-N_6(Mβ) peaks occur with a ratio of 1/0.6 and the well separated minor family members W $M_{5,4}$-$N_{3,2}$ (Mζ) and W M_3-N_5 (Mγ) can be detected in a high count spectrum, as shown for W in ◘ Fig. 18.13c.

18.4.4 Identifying the Peaks: Minor and Trace Constituents

After all major peaks and their associated minor family members and artifact peaks have been located and identified with high confidence as belonging to particular elements, the analyst can proceed to identify any remaining peaks which are now likely to be associated with minor and trace level constituents. Achieving the same degree of high confidence in the identification of lower concentration constituents is more difficult since the lower concentrations reduce all X-ray intensities so that minor family members are more difficult to detect. The situation is likely to require accumulating additional X-ray counts to improve the detectability of minor X-ray family members and increase the confidence of the assignment of elemental identification. In general, establishing the presence of a constituent at trace level is a significant challenge that requires not only collecting a high count spectrum that satisfies the limit of detection criterion but also scrupulous attention to identifying all possible minor family members and artifacts from the X-ray families of the major and minor constituents.

18.4.5 Checking Your Work

The only way to be confident that the qualitative analysis is correct to quantify the spectrum and examine the residual spectrum. When every element has been correctly identified and quantified, the analytical total should be approximately unity and there should be no obvious structure in the residual spectrum that cannot be explained through chemistry or minor chemical peak shifts. This iterative qualitative – quantitative analysis scheme to discover minor and trace elements hidden under the high intensity peaks of major constituents will covered in ► Chapter 19.

18.5 A Worked Example of Manual Peak Identification

Alloy IN100 is a complex mixture of transition and heavy elements that provides several challenges to manual peak identification:

1. ◘ Figure 18.14a shows the spectrum from 0 to 20 keV excited with $E_0 = 20$ keV. Using the KLM marker tools in DTSA II, starting at high photon energy and working downward, the first high peak encountered shows a good match to Ni K-L_3 and the corresponding Ni K-M_3 is also found at the correct ratio, as well as the Ni L-family at low photon energy. The position of the Ni K-L_3 escape peak is marked. Inspection for possible coincidence peaks does not reveal a significant population due to the low dead-time (8 %) used to accumulate the spectrum and the large number of peaks over which the input count rate is partitioned so that even the most intense peak has a relatively low count rate and does not produce significant coincidence.
2. Working down in energy (◘ Fig. 18.14b), the next peak is seen to correspond to Co K-L_3, but the Co K-M_3 suffers interference from Ni K-L_3 and only appears as an asymmetric deviation on the high energy side. Likewise, the Co L-family is unresolved from the Ni L-family.
3. The next set of peaks match Cr, as shown in ◘ Fig. 18.14c.
4. Continuing, ◘ Fig. 18.14d shows a match for the peaks of Ti, but the apparent ratio of Ti K-L_3/Ti K-M_3 is approximately 5:1, whereas the true ratio is about 10:1, which suggests that another element must be present. Expansion of this region in ◘ Fig. 18.14e reveals that V is likely to be present but with severe interference between V K-L_3 and Ti K-M_3. While the anomalous peak ratio observed for TiK-L_3/TiK-M_3 is a strong clue that another element must be present, this example shows one of the limitations of manual peak identification, namely, that peaks representing minor and trace constituents can be lost under the higher intensity peaks of higher concentration constituents as the concentration ratio becomes large. Detecting such interferences of constituents with large concentration ratios requires the careful peak-fitting procedure that is embedded in the quantitative analysis procedures described in module 19.
5. In ◘ Fig. 18.14f, the next peak group best matches the Mo L-family. This photon energy range involves possible interferences from the S K-family, the Mo L-family, and the Pb M-family. The possibility of identifying the peak group as the Pb M-family which occurs this energy range, can be rejected because of the absence of the Pb L-family, as shown in ◘ Fig. 18.14g. The possible presence of the S K-family (◘ Fig. 18.14h) is much more difficult to exclude because S cannot be effectively measured by an alternate X-ray family such as the S L-family due to the low fluorescence yield. While the shape of the peak cluster does not match S K-L_3 and S K-M_3, the presence of S can only be confidently

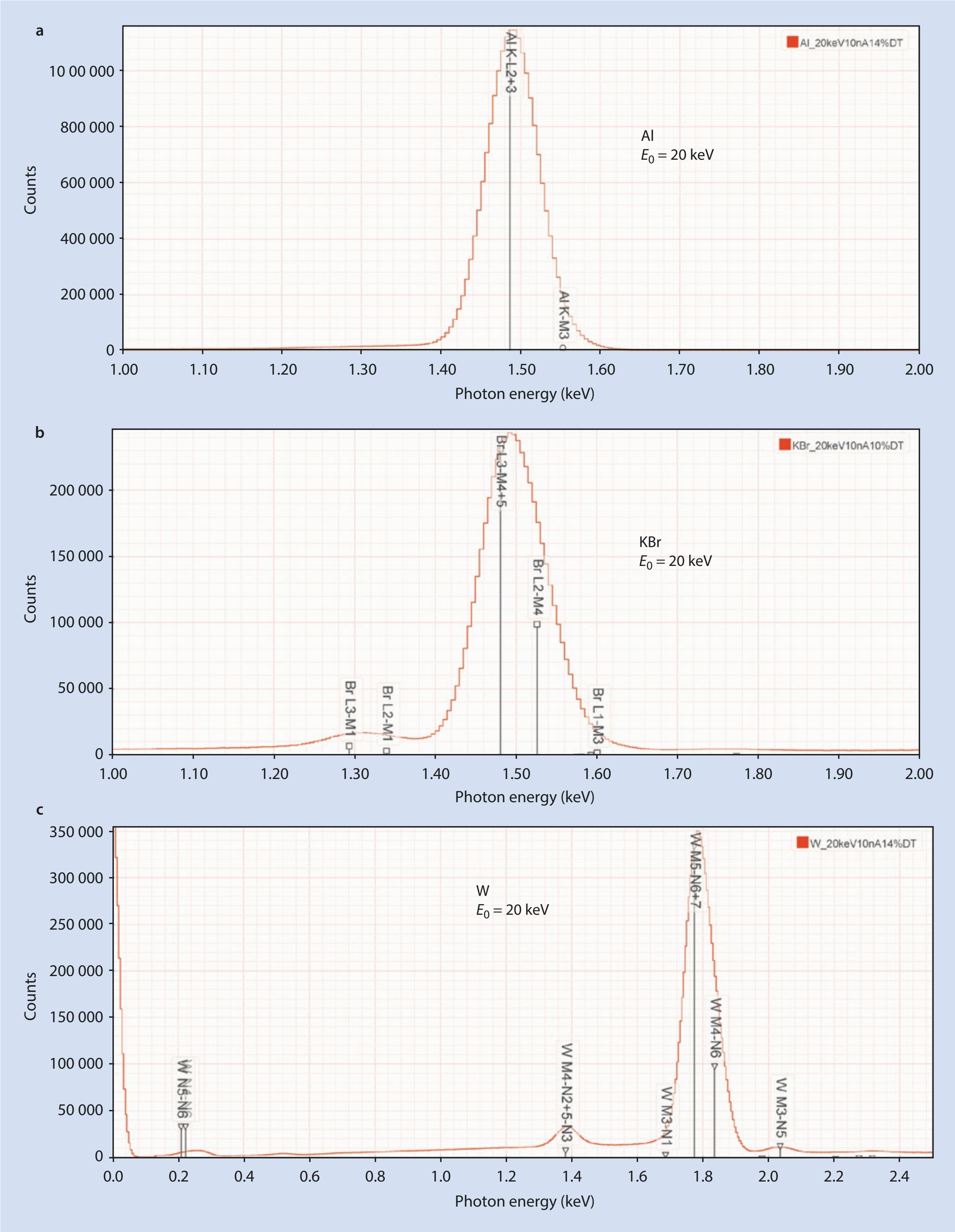

Fig. 18.13 **a** EDS spectrum of Al at $E_0 = 20$ keV; note symmetry of Al K-family peaks. **b** EDS spectrum of KBr at $E_0 = 20$ keV; note asymmetry of Br L-family peaks. **c** EDS spectrum of W at $E_0 = 20$ keV; note asymmetry of W M-family peaks

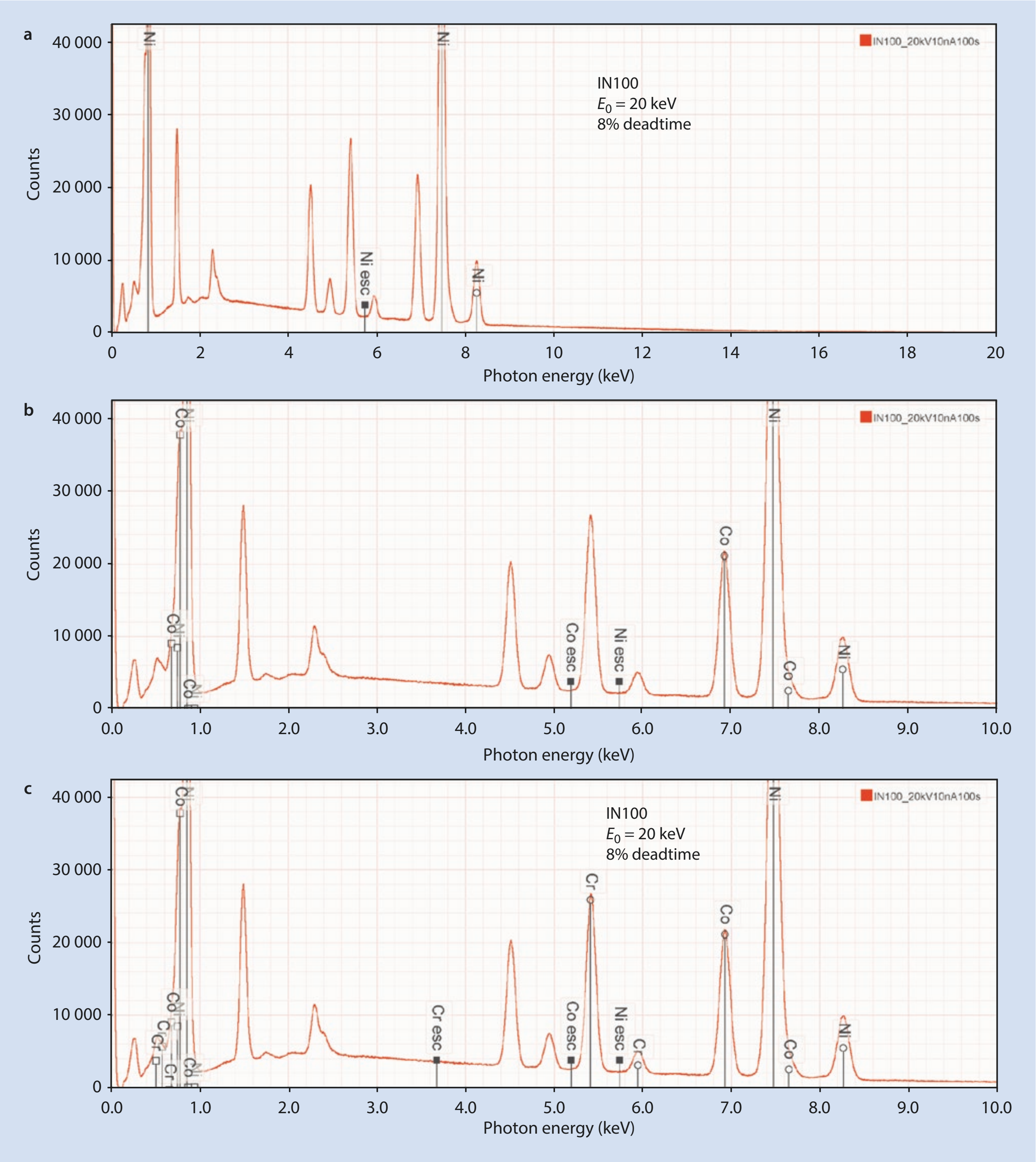

Fig. 18.14 **a** Alloy IN100 recorded with $E_0 = 20$ keV and at 8 % dead-time showing identification of Ni. **b** Identification of Co. **c** Identification of Cr. **d** Identification of Ti. **e** Identification of V. **f** Identification of Mo. **g** Rejection of Pb. **h** Possible presence of S. **i** Identification of Al. **j** Rejection of Br. **k** Identification of C. **l** Identification of Si

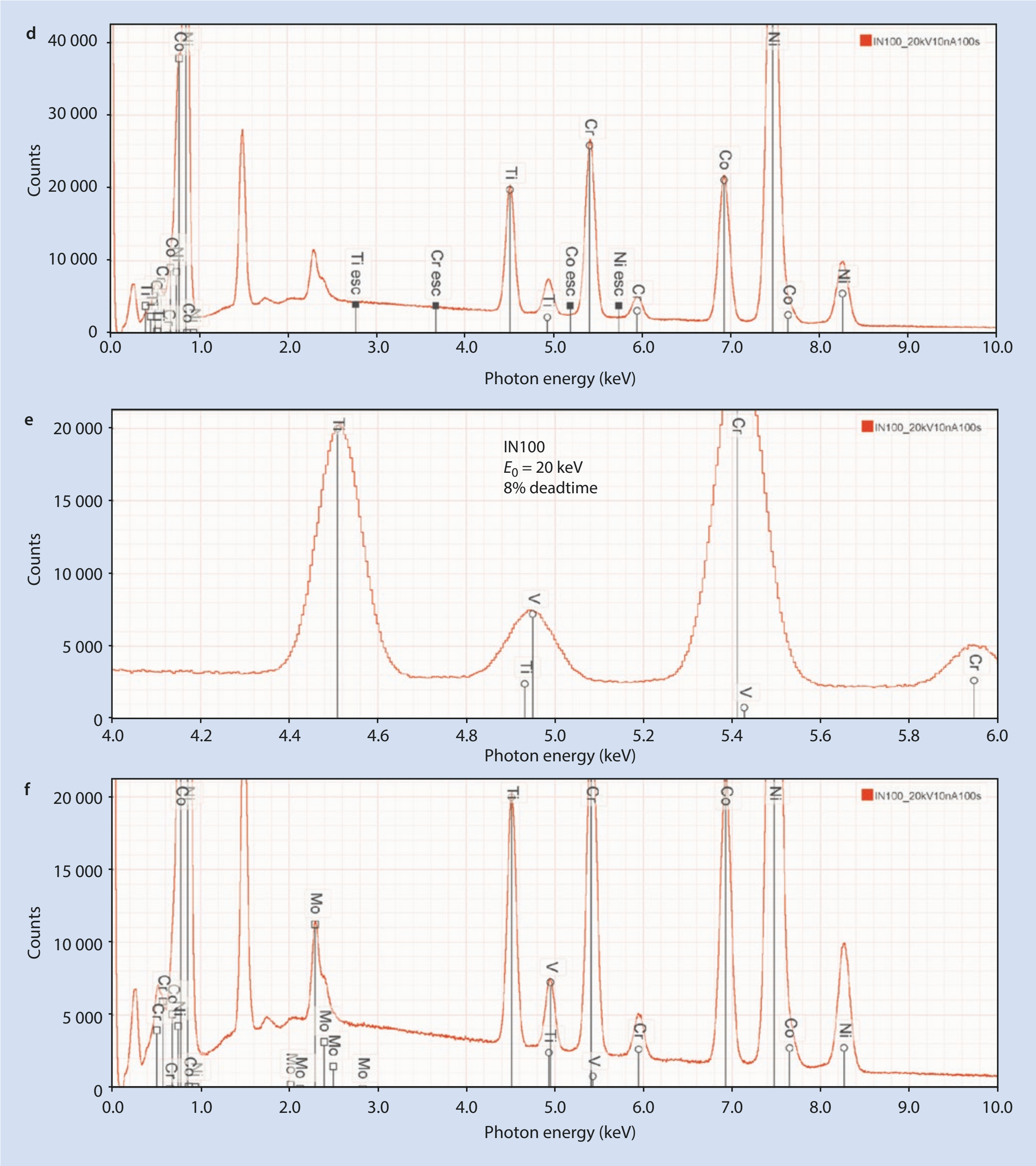

Fig. 18.14 (continued)

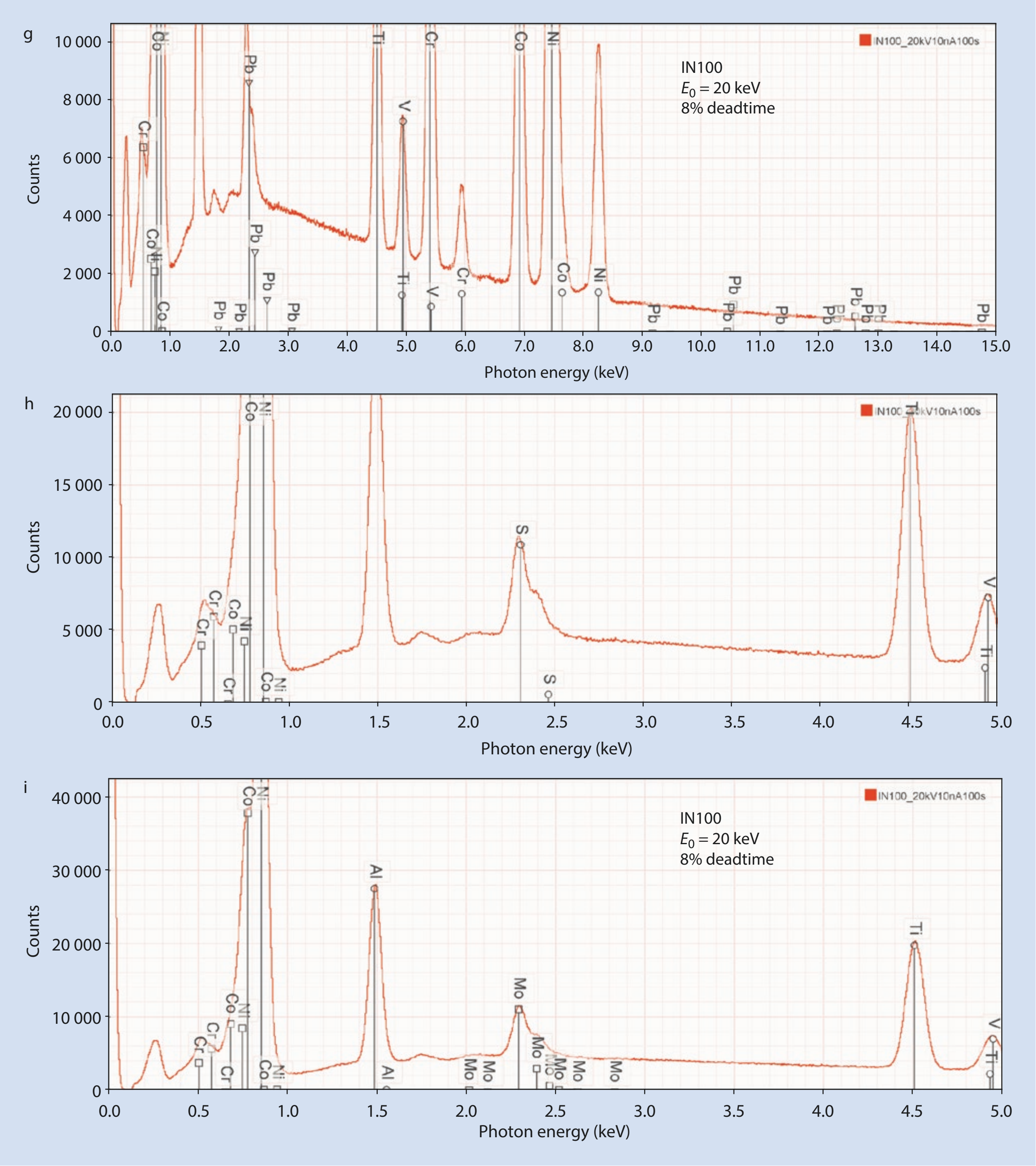

Fig. 18.14 (continued)

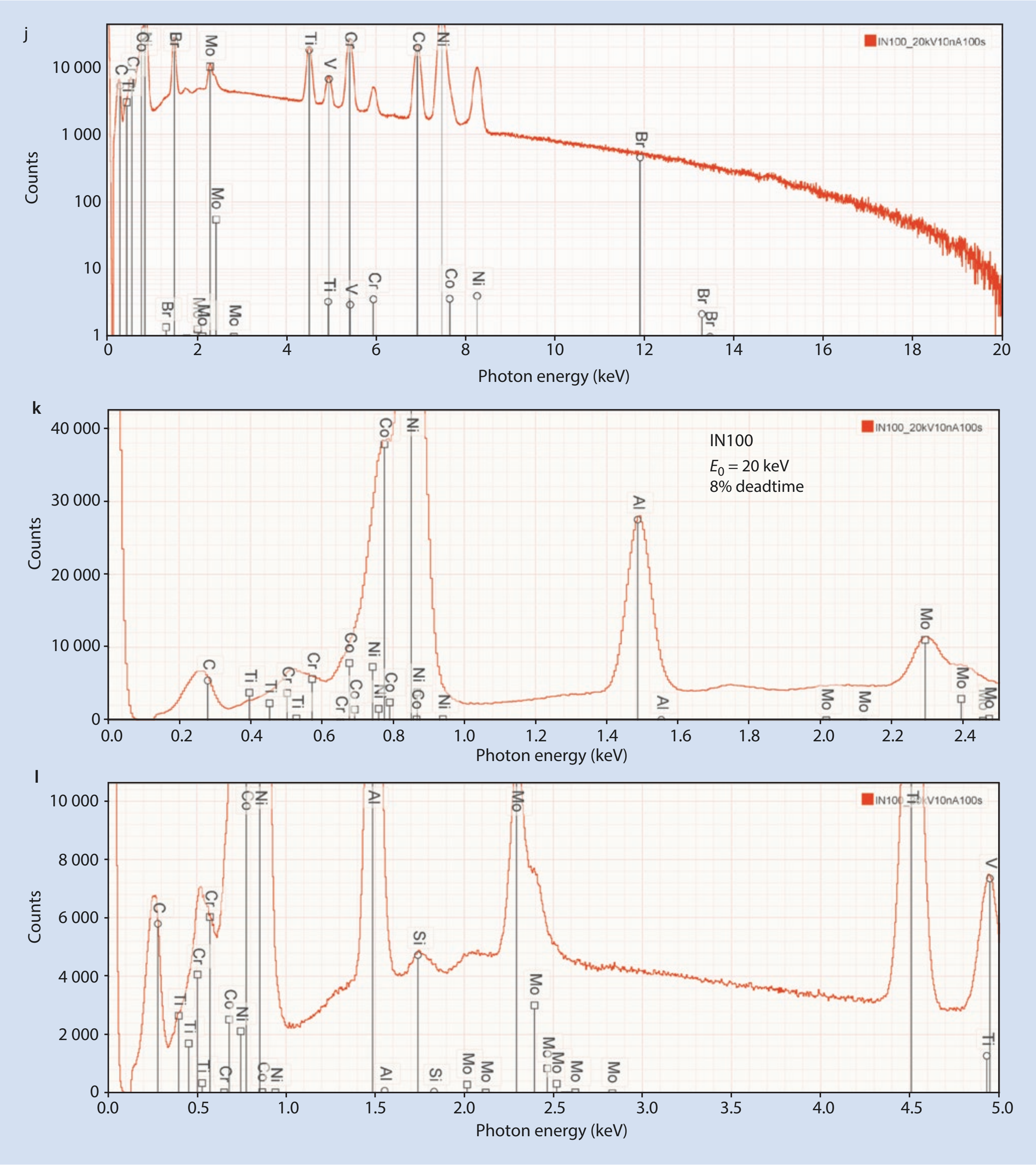

Fig. 18.14 (continued)

confirmed by peak fitting procedures during quantitative analysis.

6. The next peak matches the Al K-family (Fig. 18.14i) but in this photon energy range only one peak is available for identification. The Br L-family also fits this peak (Fig. 18.14j) but Br can be dismissed because of the absence of the Br K-family.
7. The last significant peak is found to correspond to C K (Fig. 18.14k) noting that due to the non-linearity of the photon energy scale for this detector below 400 eV, the peak is displaced to a lower energy from the ideal position.
8. Finally, inspection of the remaining low peak-to-background peaks reveals just one candidate, which corresponds to the Si K-family (Fig. 18.14l).

References

Currie LA (1968) Limits for qualitative detection and quantitative determination. Anal Chem 40:586

Newbury D (2005) Misidentification of major constituents by automatic qualitative energy dispersive X-ray microanalysis: a problem that threatens the credibility of the analytical community. Microsc Microanal 11:545

Newbury D (2007) Mistakes encountered during automatic peak identification in low beam energy X-ray microanalysis. Scanning 29:137

Newbury D (2009) Mistakes encountered during automatic peak identification of minor and trace constituents in electron-excited energy dispersive X-ray microanalysis. Scanning 31:1

Statham P (1995) Quantifying Benefits of resolution and count rate in EDX microanalysis. In: Williams D, Goldstein J, Newbury D (eds) X-ray spectrometry in electron beam instruments. Plenum, New York, pp 101–126